NANO LETTERS

2003
Vol. 3, No. 8
1025−1028

SnO_2 Nanoribbons as NO_2 Sensors: Insights from First Principles Calculations

Amitesh Maiti,*,† José A. Rodriguez,‡ Matthew Law,§ Paul Kung,† Juan R. McKinney,§ and Peidong Yang§

Accelrys Inc., 9685 Scranton Road, San Diego, California 92121, Department of Chemistry, Brookhaven National Laboratory, Upton, New York 11953, and Department of Chemistry, University of California, and Materials Science Division, Lawrence Berkeley National Laboratory, Berkeley, California 94720

Received April 17, 2003; Revised Manuscript Received May 30, 2003

ABSTRACT

SnO_2 nanoribbons with exposed (1 0 $\bar{1}$) and (0 1 0) surfaces have recently been demonstrated to be highly effective NO_2 sensors even at room temperature. The sensing mechanism is examined here through first principles density functional theory (DFT) calculations. We show that the most stable adsorbed species involve an unexpected NO_3 group doubly bonded to Sn centers. Significant electron transfer to the adatoms explains an orders-of-magnitude drop in electrical conductance. X-ray absorption spectroscopy indicates predominantly NO_3 species on the surface, and computed binding energies are consistent with adsorbate stability up to 700 K. Nanoribbon responses to O_2 and CO sensing are also investigated.

The field of nanotechnology continues to advance at a breathtaking pace, propelled by the discovery of new materials, new devices, and new phenomena. Metal oxide nanoribbon materials systems, particularly those synthesized from inexpensive SnO_2 and ZnO,[1−3] have been of great current interest because of potential applications as chemical sensors for pollutant gas species and biomolecules.[4−6] The use of single-crystalline SnO_2 nanoribbons as NO_2 sensing devices was recently demonstrated at room temperature,[7] in which the electrical conductance was found to decrease by orders of magnitude upon NO_2 adsorption. Such single-crystalline nanowire sensing elements have several advantages over conventional thin film oxide sensors: low operating temperatures, no ill-defined coarse-grain boundaries, and a high active surface-to-volume ratio.

The experimental nanoribbons were synthesized using a novel approach based on a simple thermal-deposition process.[1] Field-emission scanning electron microscopy (FE-SEM) and transmission electron microscopy revealed that the ribbons (1) possess a highly crystalline rutile structure; (2) grow tens of micrometers long in the ⟨1 0 1⟩ direction; (3) display a uniform quasi-rectangular cross section perpendicular to the growth direction; and (4) present the (1 0 $\bar{1}$) and (0 1 0) rutile planes as surface facets along the growth axis, with dimensions ranging from 80−120 nm × 10−30 nm. Rutile SnO_2 is a wide band gap (3.6 eV) *n*-doped semiconductor with the intrinsic carrier density determined by the deviation from stoichiometry, primarily in the form of oxygen vacancies.[8]

In this letter, we have carried out a first principles DFT investigation of the adsorption process of NO_2 on the exposed (1 0 $\bar{1}$) and (0 1 0) surfaces as well as the edge atoms of a SnO_2 nanoribbon. The DFT code that was used was DMol[3],[9,10] in which each electronic wave function is expanded in a localized atom-centered basis set defined on a numerical grid. We performed all-electron calculations[11] with a double numeric polarized (DNP) basis set and the gradient-corrected PBE functional.[13] Nanoribbon surfaces were represented in periodic supercells, and accurate Brillouin zone integration was performed via careful sampling of k points chosen according to the Monkhorst−Pack scheme[14] with a k-point spacing of 0.1 $Å^{-1}$. To estimate charge transfer to adatoms, we computed partial charge on each atom using the Mulliken population analysis.[15]

In bulk rutile SnO_2, the Sn atoms are octahedrally coordinated with six O neighbors, and each O atom is a 3-fold bridge between neighboring Sn centers. At both the (1 0 $\bar{1}$) and (0 1 0) surfaces, the Sn atoms lose an O neighbor,[16] thereby becoming 5-fold coordinated (Figure 1a and b). The surface O atoms become 2-fold-coordinated

* Corresponding author. E-mail: amaiti@accelrys.com.
† Accelrys Inc.
‡ Brookhaven National Laboratory.
§ University of California, and Materials Science Division, Lawrence Berkeley National Laboratory.

10.1021/nl034235v CCC: $25.00
Published on Web 06/28/2003

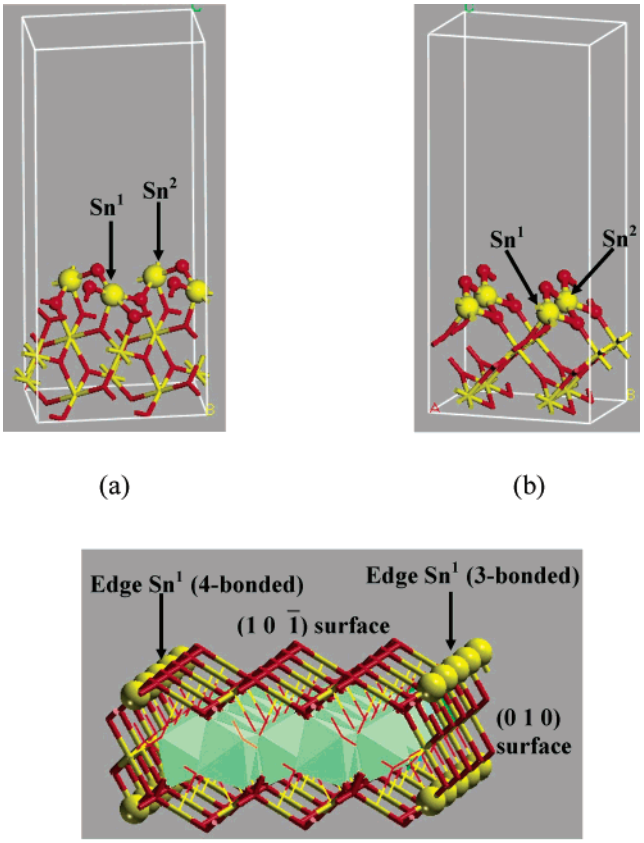

Figure 1. Simulation supercells representing exposed surfaces of a SnO_2 nanoribbon: (a) (1 0 $\bar{1}$) surface; (b) (0 1 0) surface; and (c) nanoribbon edge. For clarity, the periodic cell is not shown in c, and the interior atoms are represented by polyhedra. Surface atoms in a and b and edge atoms in c are shown in ball representation. Yellow (larger) balls and red (smaller) balls represent Sn and O atoms, respectively. Sn^1 and Sn^2 are neighboring Sn atoms connected with a bridging O and are used in Figure 2 to describe bonding configurations of adatoms schematically.

bridges connecting neighboring surface Sn atoms (Figure 1a and b). Both surfaces were represented by three layers of Sn, each layer sandwiched between two O layers. The bottom SnO_2 layer was fixed to simulate the presence of several bulklike layers in the actual sample. To reduce the interaction with periodic images, the surface unit cell was doubled in the direction of the smaller surface lattice constant, and a vacuum of 15 Å was placed normal to the surface. To simulate nanoribbon edges (i.e., lines of intersection of (1 0 $\bar{1}$) and (0 1 0) planes), a structure such as that shown in Figure 1c was embedded in a periodic supercell with the smallest repeat period (5.71 Å) along the length of the ribbon and a vacuum of 15 Å normal to both the (1 0 $\bar{1}$) surface (*y* axis) and the (0 1 0) surface (*x* axis). At the nanoribbon edges, the Sn atoms can be either 3-fold- or 4-fold-coordinated (Figure 1c).

Table 1 summarizes the computed binding energy and charge transfer for all important adatom structures resulting from NO_2 adsorption on defect-free (1 0 $\bar{1}$) and (0 1 0) surfaces and the edges.[17] In addition, the first two rows describe structures resulting from the adsorption of O_2 and

Table 1. Binding Energy and Charge Transfer for Various Adatom Configurations on Defect-Free (1 0 $\bar{1}$), (0 1 0), and Edges of an SnO_2 Nanoribbon[a]

surface	adatom structure	binding energy[b] (kcal/mol)	net charge transfer (el)
(1 0 $\bar{1}$)	$[O_2]$[c]	1.4	0.00
	$[CO]_{2,Sn,O}$	12.9	+0.10
	$[NO_2]_1$	11.2	−0.17
	$[NO_2]_2$	13.8	−0.17
	$[NO_2]_{2,Sn,O}$	2.8	+0.05
	$[NO_3]_1$	14.3	−0.30
	$[NO_3]_2$	25.5	−0.41
(0 1 0)	$[NO_2]_1$	6.5	0.03
	$[NO_2]_2$	9.7	0.02
	$[NO_3]_1$	9.4	−0.24
	$[NO_3]_2$	10.8	−0.30
edge (3-bonded)	$[NO_2]_{2,1}$	17.1	−0.41
	$[NO_3]_{2,1}$	29.3	−0.48
edge (4-bonded)	$[NO_2]_{2,1}$	18.6	−0.34
	$[NO_3]_{2,1}$	31.6	−0.48

[a] Bonding geometries of various structures are graphically illustrated in Figure 2. [b] Binding energies of all $[NO_3]$ structures are defined with regard to an NO_3 radical. [c] Spin triplet.

CO on (1 0 $\bar{1}$). Oxygen forms a weakly bonded[18] physisorbed structure $[O_2]$ in a spin-triplet configuration with the O atoms symmetrically on top of neighboring Sn atoms. More importantly, there is no charge transfer between the oxygen molecule and the surface. Thus, in the absence of structural defects (e.g., surface O vacancies), atmospheric O_2 should not affect the sensor performance of SnO_2 nanoribbons. However, the C atom of CO forms two single bonds to the surface—one to a surface Sn and a second to a bridging O on the surface—while retaining a double bond to its own O atom. The resulting $[CO]_{2,Sn,O}$ structure (Figure 2) has a binding energy of ∼13 kcal/mol. There is a net transfer of 0.1 electron from the CO to the nanoribbon surface, which should lead to an *increase* in nanoribbon electrical conductance, in agreement with recent experimental observations.[5]

The adsorption of NO_2 offers a more complicated scenario. On defect-free (1 0 $\bar{1}$) or (0 1 0) surface, it can either form an $[NO_2]_1$ structure single bonded to a Sn or a bidentate $[NO_2]_2$ structure with single bonds to neighboring Sn atoms[20] (Figure 2). On comparing $[NO_2]$ structures on (1 0 $\bar{1}$) versus those on (0 1 0), we find that (i) the binding energies are higher on the (1 0 $\bar{1}$) surface by 4−5 kcal/mol; (ii) bidentate structure $[NO_2]_2$ is more stable than the single bonded $[NO_2]_1$ structure by 2−3 kcal/mol;[21] and (iii) there is significant electron transfer from the nanoribbon to the $[NO_2]$ structures on (1 0 $\bar{1}$) but charge transfer is very small on (0 1 0).[22] On each surface, the $[NO_2]_2$ structure is only 2.6−3.2 kcal/mol more stable than the $[NO_2]_1$ structure. Thus, even at room temperature, $[NO_2]_2$ should readily be able to break one of the bonds, and the resulting $[NO_2]_1$ should rotate and rebond to a different neighboring Sn. The above process constitutes a "step" in a random walk by NO_2 on the surface. On both surfaces, the random walk should occur along well-defined rows of Sn atoms. Because the binding energies are lower on the (0 1 0) surface, mobility is expected to be higher on this surface as well.

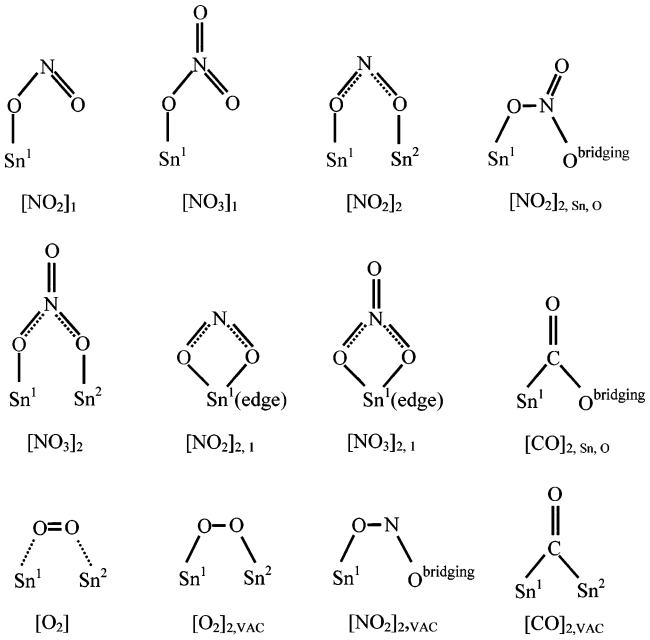

Figure 2. Schematic representation of adatom structures listed in Tables 1 and 2. Structure names follow the convention $[\ ]_1$, one single bond to a surface Sn; $[\ ]_2$, two single bonds, each to a different (and neighboring) Sn atom; $[\ ]_{2,Sn,O}$, one bond to Sn and the other to O; and $[\ ]_{2,1}$, two single bonds, both to the same Sn atom (possible only at edges). The first nine structures are considered in Table 1. The last three structures occur at surface O vacancies and are considered in Table 2. In $[NO_2]_{2,vac}$, the $O^{bridging}$ comes from NO_2 and fills a preexisting O vacancy. For visual clarity, only adatoms and reacting Sn and bridging O atoms are shown. All calculations were actually performed in periodic supercells of Figure 1a−c.

The picture drastically changes, producing unexpected chemistry, when a second NO_2 is incident on an already adsorbed $[NO_2]_2$ either from the gas phase or through surface diffusion in a manner described in the preceding paragraph. On (1 0 $\bar{1}$), an oxygen atom spontaneously breaks away from the second NO_2 and converts the preexisting $[NO_2]_2$ into an $[NO_3]_2$ structure with a much higher binding energy of 25.5 kcal/mol. The resulting NO molecule binds weakly to the breakaway oxygen and can either desorb from the surface or get incorporated at a neighboring Sn site not occupied by another NO_2.[23] By breaking an Sn−O bond, the $[NO_3]_2$ can lead to an $[NO_3]_1$ structure. However, unlike $[NO_2]$, the difference between the bidentate and single-bonded $[NO_3]$ structures is much higher, 11.2 kcal/mol. Therefore, the $[NO_3]$ species is not expected to be mobile on the (1 0 $\bar{1}$) surface. The $[NO_3]_2$ structure also takes up a significant amount of charge from the surface, ∼0.4 electrons, which should lead to a significant drop in electrical conductance. On (0 1 0), the $[NO_3]_1$ and $[NO_3]_2$ structures also take up significant electronic charge from the surface. However, there are two major differences: (i) the binding energies are relatively much lower, especially for $[NO_3]_2$ and (ii) the difference in energy between $[NO_3]_1$ and $[NO_3]_2$ is only 1.4 kcal/mol, implying that the $[NO_3]$ species should be mobile on the (0 1 0) surface.[24] As compared to those on flat surfaces, charge transfer and binding energies for both $[NO_2]$ and $[NO_3]$ species are higher at the nanoribbon edges, with the 4-fold-coordinated edge atoms supporting slightly more strongly bound structures. It is interesting that only the edges can support structures such as $[NO_2]_{2,1}$ and $[NO_3]_{2,1}$, bonded to a single Sn site through two separate Sn−O bonds.

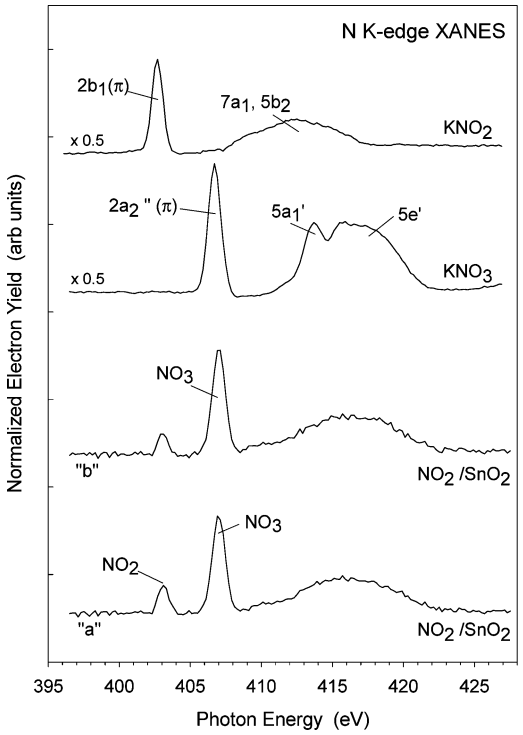

Figure 3. N K-edge XANES spectra acquired after exposing nanoribbons of SnO_2 to NO_2 at 300 K. Traces "a" and "b" correspond to two different nanoribbon samples. Included are the corresponding spectra for KNO_2 and KNO_3. The assignment of the features in these spectra is discussed in refs 27 and 28.

To confirm the high stability of the $[NO_3]$ species on SnO_2 nanoribbons, we used X-ray absorption near-edge spectroscopy (XANES). Nitrogen K-edge XANES spectra (resolution ∼0.5 eV) were recorded at beamline U7A of the National Synchrotron Light Source at Brookhaven National Laboratory[27,28] in the electron yield mode by using a channeltron multiplier near the sample surface. Figure 3 displays the room-temperature N K-edge spectra for two nanoribbon samples[29] alongside two common standards (KNO_2, KNO_3). It indicates the coexistence of NO_2 and NO_3 species on the surface of both nanoribbons. NO_3 was clearly the dominant component, with the relative amount of NO_2 varying between 20 and 30%. Thermal heating to 400 K led to the desorption of all of the adsorbed NO_2, but a detectable coverage of NO_3 remained up to around 700 K, probably a consequence of nitrate molecules bonded to the edges of the nanoribbons.

Finally, the effects of surface oxygen vacancies (on the (1 0 $\bar{1}$) surface) were examined, as summarized in Table 2. Oxygen interacts strongly with a vacancy, forming a peroxide-bridge structure $[O_2]_{2,vac}$. Computed charge transfer indicates that $[O_2]_{2,vac}$ should lead to a significant drop in nanoribbon conductance, in agreement with recent experiments on ZnO nanowires.[30] The binding strength of NO_2 at an O vacancy is also significantly higher than on a defect-free surface because one of the NO_2 oxygens fills the vacancy, thereby forming the $[NO_2]_{2,vac}$ structure (Figure 2). However, NO can easily desorb from this geometry ($E_{desorption}$

Table 2. Binding Energy and Charge Transfer for Various Adatoms at an Oxygen-Vacancy Site on the (1 0 $\bar{1}$) Surface of an SnO_2 Nanoribbon[a]

adatom structure	binding energy (kcal/mol)	net charge transfer (el)
$[O_2]_{2,vac}$	38.5	−0.88
$[NO_2]_{2,vac}$	41.4[b]	−0.51
$[CO]_{2,vac}$	6.1	−0.10

[a] See Figure 2 (bottom three structures) for a schematic description. [b] The desorption energy of NO (with O vacancy filled up) is ∼1.8 kcal/mol.

≈ 1.8 kcal/mol), thus leaving behind a defect-free surface.[31] Compared to other adsorbates, CO has weaker binding to vacancies, and CO sensing should be dominated by its adsorption on flat surfaces.

Acknowledgment. A.M. thanks Accelrys Inc. for supporting this work. J.A.R. was financed by the U.S. DOE (Chemical and Materials Sciences Divisions). P.Y. is an A. P. Sloan Research Fellow. Work at UC, Berkeley was supported by the NSF. Work at LBL was supported by the Division of Materials Science, Office of Science, Basic Energy Sciences of the U.S. DOE. We thank the National Center of Electron Microscopy for the use of their facilities.

References

(1) Dai, Z. R.; Pan, Z. W.; Wang, Z. L. *Solid State Commun*. **2001**, *118*, 351.
(2) Huang, M.; Wu, Y.; Feick, H.; Tran, N.; Weber, E.; Yang, P. *Adv. Mater*. **2001**, *13*, 113.
(3) Huang, M.; Mao, S.; Feick, H.; Yan, H.; Wu, Y.; Kind, H.; Weber, E.; Russo, R.; Yang, P. *Science* **2001**, *292*, 1897.
(4) Cui, Y.; Wei, Q.; Park, H.; Lieber, C. M. *Science* **2001**, *293*, 1289.
(5) Comini, E.; Faglia, G.; Sberveglieri, G.; Pan, Z.; Wang, Z. L. *Appl. Phys. Lett.* **2002**, *81*, 1869.
(6) Favier, F.; Walter, E. C.; Zach, M. P.; Benter, T.; Penner, R. M. *Science* **2001**, *293*, 2227.
(7) Law, M.; Kind, H.; Kim, F.; Messer, B.; Yang, P. *Angew. Chem., Int. Ed*. **2002**, *41*, 2405.
(8) Founstadt, C. G.; Rediker, R. H. *J. Appl. Phys.* **1971**, *42*, 2911.
(9) More details about DMol^3 can be found at http://www.accelrys.com/mstudio/DMol3.html.
(10) Delley, B. *J. Chem. Phys.* **1990**, *92*, 508. Delley, B. *J. Phys. Chem.* **1996**, *100*, 6107. Delley, B. *Int. J. Quantum Chem.* **1998**, *69*, 423. Delley, B. *J. Chem. Phys.* **2000**, *113*, 7756.
(11) To estimate the relativistic effects due to Sn, we have also repeated a few calculations with semilocal pseudopotentials[12] that were recently developed for DMol^3, which contains scalar relativistic corrections. The changes in all of the computed adsorption energies were small, less than 0.5 kcal/mol.
(12) Delley, B. *Phys. Rev. B* **2002**, *66*, 155125.
(13) Perdew, J. P.; Burke, K.; Ernzerhof, M. *Phys. Rev. Lett.* **1996**, *77*, 3865.
(14) Monkhorst, H. J.; Pack, J. D. *Phys. Rev. B* **1976**, *13*, 5188.
(15) Szabo, A.; Ostlund, N. S. *Modern Quantum Chemistry*; Dover: New York, 1996; p 151.
(16) If we terminate the surface at a dangling O layer such that all surface Sn atoms remain octahedrally coordinated, then a pair of neighboring dangling O atoms break away from their Sn neighbors and readily form a spin-triplet O_2 molecule that is weakly physisorbed on the top of the Sn atoms (structure $[O_2]$ in Table 1).
(17) To start with, all oxygen vacancies[8] are assumed to be in the bulk of the oxide. However, the effect of surface O vacancies can be substantial and are considered later in the text.
(18) From previous experience,[19] we can estimate the accuracy of DMol^3-computed binding energies to be within 0.5 kcal/mol with the parameter settings used in this work. Therefore, weak binding energies, or small differences between binding energies, should be treated with some error bars in mind. However, such an error bar is not expected to change any of our main conclusions.
(19) Maiti, A.; Sierka, M.; Andzelm, J.; Golab, J.; Sauer, J. *J. Phys. Chem A* **2000**, *104*, 10932.
(20) NO_2 structures involving a bridging oxygen (e.g., $[NO_2]_{2,Sn,O}$) are not very stable and do not involve large charge transfers.
(21) Because $[NO_2]_1$ and $[NO_2]_2$ can readily convert into one another without any significant atomic rearrangement, equilibrium statistics at room temperature would predict almost all $[NO_2]$ structures to be in the bidentate form. However, $[NO_2]_1$ could potentially act as a metastable structure, leading to a random walk of NO_2 on the surface.
(22) A net electron transfer from NO_2 to the (0 1 0) surface should be taken with some reservation because of approximations involved in the definition of the Mulliken charge.[15]
(23) NO adsorbed at the neighboring Sn site forms a structure such as $[NO_2]_{2,vac}$ (Figure 2) with a weak binding energy of 1.8 kcal/mol.
(24) Insight into binding-energy and charge-transfer differences between the two surfaces can be obtained from the relative positions of the highest occupied molecular orbital (HOMO).[25] These are at −6.3, −7.2, −6.0, and −8.1 eV, respectively, for the (1 0 $\bar{1}$) surface, the (0 1 0) surface, isolated NO_2, and isolated NO_3. The HOMO is fully occupied for the surfaces and half-occupied for the molecules (odd number of electrons). Thus, upon NO_x adsorption, any electron transfer should occur from the surface HOMO to the half-occupied HOMO of the adsorbate.[26] The relative positions of these levels would clearly explain (i) almost no charge transfer to $[NO_2]$ on the (0 1 0) surface; (ii) higher charge transfer to $[NO_3]$ as compared to that to $[NO_2]$ on both surfaces; and (iii) higher binding on the (1 0 $\bar{1}$) surface, especially for an $[NO_3]$ species.
(25) For periodic surfaces, this corresponds to the top of the valence band.
(26) The LUMOs (lowest unoccupied molecular orbitals or bottom of the conduction band) of all four systems are several electronvolts higher and are not considered in this discussion.
(27) Rodriguez, J. A.; Jirsak, T.; Sambasiban, S.; Fischer, D.; Maiti, A. *J. Chem. Phys.* **2000**, *112*, 9929.
(28) Rodriguez, J. A.; Jirsak, T.; Liu, G.; Hrbek, J.; Dvorak, J.; Maiti, A. *J. Am. Chem. Soc.* **2001**, *123*, 3597.
(29) Both samples were removed from the air and exposed to 50 Torr of NO_2 at 300 K for 10 min in a reaction cell before recording the XANES data.
(30) Kind, H.; Yan, H.; Law, M.; Messer, B.; Yang, P. *Adv. Mater*. **2002**, *14*, 158.
(31) Repeated cycles of NO_2 sensing are thus expected to decrease the number of surface oxygen vacancies and degrade the O_2-sensing quality of the nanoribbon. This could also lead to signal drift in the practical use of such sensing elements.

NL034235V